WIND AND TEMPERATURE INDUCED EFFECTS ON MESOSPHERIC ION COMPOSITION AND INFERRED MINOR CONSTITUENTS

E. Kopp

Physikalisches Institut, University of Bern
Sidlerstr. 5, CH-3012 Bern, Switzerland

C.R. Philbrick

Air Force Geophysics Laboratory,
Hanscom AFB, Mass. 01731, USA

ABSTRACT

The positive ion composition, temperature and wind profiles were measured independently in salvo B and A2 of the 1980 Energy Budget Campaign above Kiruna. Ion chemical models of the D-region predict a strong temperature dependence for the density distribution of the proton hydrates with different hydration order. Mesospheric temperature profiles derived from a steady state ion chemical model are compared with measured scale height temperature from the accelerometer instrument falling sphere experiments.

The effect of strong horizontal neutral air transport and ion drag became evident in the total positive ion density profiles, derived from the ion mass spectrometer measurements in salvo B and A2. The nitric oxide profiles, inferred from the ion composition measurements, reveal a pronounced density depletion at 97 km in salvo B and at 93 km in salvo A2. In both cases the features correlate with regions of high wind and may result from transport effects on the nitric oxide.

1. INTRODUCTION

Results of the positive and negative ion composition measurements in the altitude range 60 - 100 km have revealed considerable variations depending on different seasons, geomagnetic latitude and solar activity (Ref. 1). A part of the variation is related to the ion production of the lower ionosphere from direct ionization of NO and O_2 ($^1\Delta_g$) by solar UV radiation. The more important effects causing a change of ion compositions is due to density variations of specific neutral species such as O, NO, odd hydrogen, H_2O and temperature. Global variation of mesospheric nitric oxide, atomic oxygen and hydrogen compounds is mainly controlled by meteorological conditions and through interaction processes of precipitated particles with the lower thermosphere and mesosphere. Seasonal and geographic variability of thermospheric nitric oxide became evident from the Explorer C satellite (Ref. 2) showing maximum densities within the auroral oval due to enhanced nitric oxide production from energetic particles. The main seasonal mesospheric nitric oxide density variability is determined by different vertical transport by eddy diffusion (Ref. 3). The seasonal variability of mesospheric atomic oxygen and ozone concentration is also evident from the total sodium content showing a general enhancement of sodium in wintertime (Ref. 4). The sensitivity of these long living trace gases in the mesosphere to meridional transport and vertical eddy diffusion is demonstrated in the two dimensional model by Garcia and Solomon (Ref. 5).

The European Energy Budget Campaign had several coordinated launches of different payloads from Kiruna and Andoya in November/December 1980. Four major salvos were launched in conditions with low, medium and high magnetic activities named salvo C, B and A respectively. The conditions of medium and high auroral activities are favourable for a study of transport of minor constituents and the effect on temperature, ion composition and energy transport.

On the 16th November 1980 two rockets named E11-A and E6-A were launched from Esrange Kiruna about 57 minutes apart at 0350 UT and 0447 UT respectively as part of 12 rockets of salvo B with medium magnetic activity and Joule heating. The same two rocket payloads were also launched from Esrange on 30th November (E11-A) and 1st December (E6-A) 1980 as part of a series of ten rockets within salvo A2. Salvo A2 had a strong magnetic activity with an accumulated Joule heating of 74.3×10^4 [$\gamma^2 \cdot h$]. The E11-A of salvo A2 was launched first at

Sixth ESA Symposium on European rocket & balloon programmes (ESA SP-183), 41 – 46

23.44.30 UT at the time of maximum horizontal magnetic field variation (ΔX = 600 nT). The E6-A flight was 24.5 minutes later. The instruments of the E11-A payload from the Universities of Illinois and Bern measured electron densities, the energetic particle flux and the positive ion composition at altitudes above 60 km. The falling sphere experiment of the Air Force Geophysical Laboratory in Hanscom on the E6-A payload gave results on total density, temperature and horizontal wind velocities.

In this paper effects of horizontal wind and temperature on the nitric oxide density profile inferred from the ion composition measurements will be presented and a comparison of the temperature derived from the distribution of proton hydrates and the falling sphere experiment is made.

The complete results of the E11-A ion composition measurements are published by Kopp et al. (Ref. 6), Schmidlin et al. (Ref. 7) and Philbrick et al. (Ref. 8).

2. THE ROCKET EXPERIMENTS

The E11-A payload was launched on a Taurus-Orion motor and measurements of positive ions were obtained between altitudes of about 60 km and 170 km on ascent of the rocket flight. The mass spectrometer was mounted on the front of the payload and ambient ions are accelerated with a bias potential of - 3 V on a cone and sampled through an orifice of 2 mm in diameter on the tip of the cone. The spectrometer is a magnetic type mass spectrometer equipped with two electron multiplier detectors. The mass range of 14 - 180 amu is scanned with a scan speed of 0.385s per octave. A more detailed instrument description is given by Kopp et al. (Ref. 9). The active falling sphere experiment was mounted under the nose cone of the E6-A payload launched on Nike-Orion motors. A three-axis piezoelectric accelerometer in the center of the 25 cm diameter sphere measures atmospheric density and horizontal wind velocities. Temperature profiles are inferred in the altitude range of 50 to 150 km. The sphere with its own telemetry and tracking system is released from the payload on ascent at about 70 km altitude. The details of the instrument are published by Philbrick et al. (Ref. 10).

3. NITRIC OXIDE

The determination of nitric oxide from ion composition results in the lower ionosphere at high latitudes has been developped by Swider and Narcisi (Ref. 11). In Fig. 1 the reaction scheme of the primary ions to the observed main ions O_2^+ and NO^+ is shown. The variability of the O_2^+ to NO^+ density ratio at different altitudes and different geomagnetic conditions

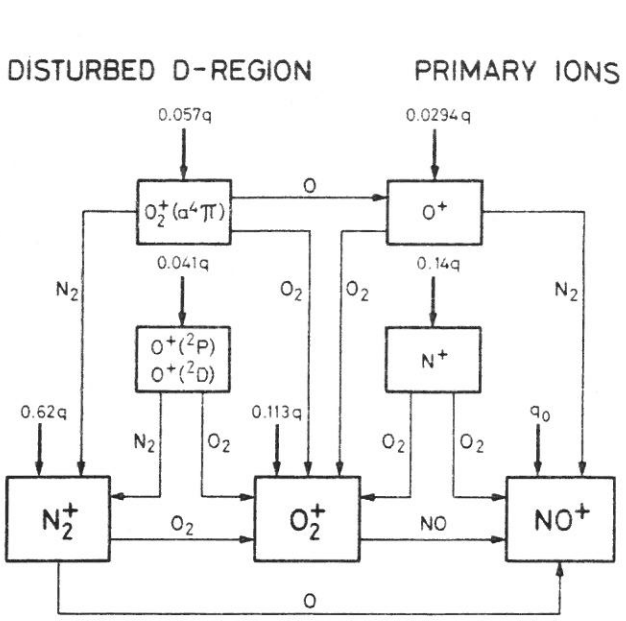

Fig. 1: Reaction scheme of primary ions in the high latitude disturbed D-region. q is the total electron-ion pair production precipitated particles and q_o is the direct ioniproduction of NO^+ by ionization of NO with the Lyman-α UV-radiation.

arises mainly due to the charge transfer reaction $O_2^+ + NO \rightarrow NO^+ + O_2$. In the altitude range of 85 - 100 km the loss of N_2^+ is through reaction $N_2^+ + O_2 \rightarrow O_2^+ + N_2$ and above 100 km the reaction of N_2^+ with atomic oxygen becomes important. The relative ionic productions by energetic particles are: 62 % (N_2^+), 17 % (O_2^+), 14 % (N^+) and 7 % (O^+), identical to those of Swider and Narcisi (Ref. 11). The reaction rate constants used for the NO model of Fig. 1 are summarized in Table 1. The total ion-electron pair production is determined above 85 km from the loss of O_2^+ and NO^+ by dissociative electron recombination. The inferred nitric oxide density profiles of salvo B and A2 are given in Fig. 2 and Fig. 3 respectively in the altitude range of 85 - 120 km. The atomic oxygen density profiles were taken from von Zahn et al. (Ref. 12) and total density and temperature from the falling sphere experiment.

The altitude resolution of the nitric oxide profiles of salvo B and A2 are of the order of one kilometer, comparable to the flight distance of the rocket within a typical scan period of the mass spectrometer. The maximum NO densities of salvo B are between $2.5 - 3.5 \times 10^{14}$ m^{-3} at altitudes between 106 - 110 km (Fig. 2). A five times higher maximum density of 2×10^{15} m^{-3} was found in the salvo A2 at 100 km, about 8 km lower compared to the maximum density values of salvo B (Fig. 3). In both flights a distinct density minimum of nitric oxide is evident at 97 km in salvo B and at 93 km in salvo A2. Below 85 km the loss of O_2^+ and

ALTITUDE (km)

Table 1. Reactions for the nitric oxide model

	Reaction		Reaction constant ($cm^3 s^{-1}$)	Reference
1.	$O_2^+ + e$	$\rightarrow O + O$	$1.9\times10^{-7}\,(\frac{300}{T})^{1/2}$	1)
2.	$NO^+ + e$	$\rightarrow N + O$	$2.3\times10^{-7}\,(\frac{300}{T})^{1/2}$	1)
3.	$O^+ + O_2$	$\rightarrow O_2^+ + O$	$1.9\times10^{-11}\,(\frac{300}{T})^{0.4}$	2)
4.	$O^+ + N_2$	$\rightarrow NO^+ + N$	$1.2\times10^{-12}\,(\frac{300}{T})$	3)
5.	$O^+(^2P,^2D) + O_2$	$\rightarrow O_2^+ + O$	7×10^{-10}	4)
6.	$O^+(^2P,^2D) + N_2$	$\rightarrow N_2^+ + O$	8×10^{-10}	4)
7.	$N_2^+ + O$	$\rightarrow NO^+ + N$	$1.4\times10^{-10}\,(\frac{300}{T})^{0.44}$	3) 5)
8.	$N_2^+ + O_2$	$\rightarrow O_2^+ + N_2$	$5.0\times10^{-11}\,(\frac{300}{T})^{0.8}$	3)
9.	$N^+ + O_2$	$\rightarrow NO^+ + O$	2.6×10^{-10}	6)
10.	$N^+ + O_2$	$\rightarrow O_2^+ + N$	3.1×10^{-10}	6)
11.	$O_2^+(a^4\pi) + O$	$\rightarrow O^+ + O_2$	5.0×10^{-10}	3)
12.	$O_2^+(a^4\pi) + O_2$	$\rightarrow O_2^+ + O_2$	3.0×10^{-10}	3)
13.	$O_2^+(a^4\pi) + N_2$	$\rightarrow N_2^+ + O_2$	4.0×10^{-10}	3)
14.	$O_2^+ + NO$	$\rightarrow NO^+ + O_2$	4.4×10^{-10}	7)

1) Mul, P.M. and J. Wm. Mc.Gowan (1979), J.Phys.B. Atom. Molec.Phys., 12, 1591
2) Lindinger, W., F.C. Fehsenfeld, A.L. Schmeltekopf and E.E. Ferguson (1974), J.Geophys.Res. 79, 4753
3) Swider, W. and R.S. Narcisi (1977), Planet. Space Sci., 25, 103
4) Johnsen, R., and M.A. Biondi (1980), J. chem.Phys. 73, 190
5) Abdou, W.A., D.G. Torr, P.G. Richards and M.R. Torr (1982), J.Geophys. Res. 87, 6324
6) Smith, D., N.G. Adams, and T.M. Miller (1978), J.chem.Phys. 69, 308
7) Lindinger, W., D.L. Albritton, F.C. Fehsenfeld, and E.E. Ferguson (1975), J.Geophys.Res. 80, 3725

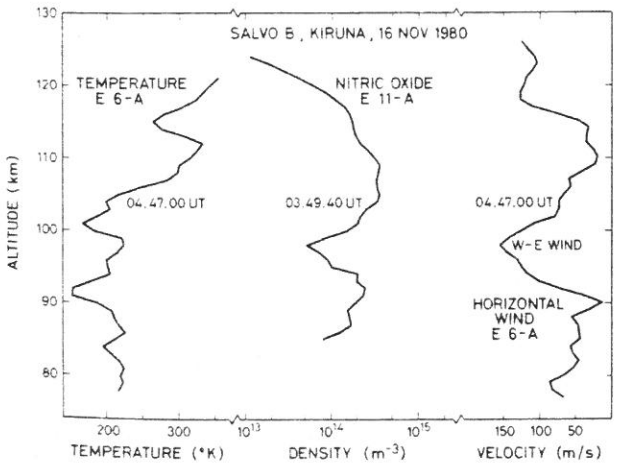

Fig. 2: Altitude profiles of the nitric oxide density inferred from positive ion composition measurements on the E11-A payload in salvo B. The profiles of atmospheric neutral temperature and total horizontal wind velocity are from the measurements of the active falling sphere experiment, launched on the E6-A payload in the same salvo B 57 minutes later.

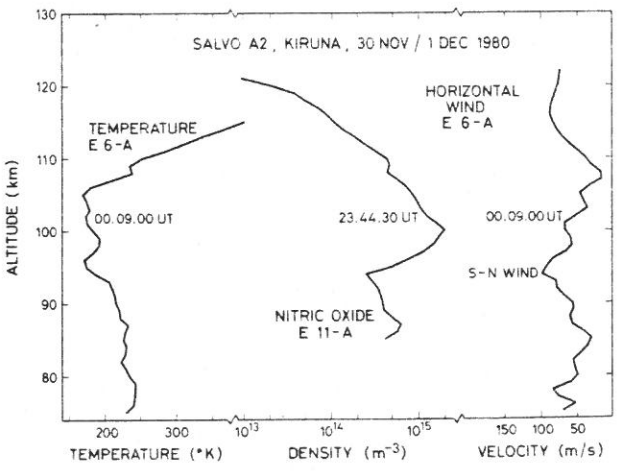

Fig. 3: Altitude profiles of the nitric oxide density inferred from positive ion composition measurements on the E11-A payload in salvo A2. The profiles of atmospheric neutral temperature and total horizontal wind velocity are from the measurements of the active falling sphere experiment, launched on the E6-A payload in the same salvo A2 24 minutes later.

and NO^+ in three body type reactions leading to cluster ions cannot any longer be neglected and the calculated nitric oxide densities become more uncertain and are thus not shown in Figs. 2 and 3.

4. EFFECT OF TRANSPORT AND TEMPERATURE ON MESOSPHERIC NITRIC OXIDE

Previous nitric oxide densities inferred from mass spectrometric measurements at various seasons and latitudes by Swider (Ref. 13) and Arnold (Ref. 1) show large density variations at mesospheric heights within 5×10^{12} m^{-3} - 2×10^{15} m^{-3}. A general density decrease is evident in the 80 - 90 km region, with some exceptions found at high latitudes and during winter anomalies. The variability and strong nitric oxide gradients in the mesosphere suggest that mainly transport effects are the controlling factors of the mesospheric NO, especially since no significant production of nitric oxide is known in the mesosphere. Nevertheless, due to limited height resolution of the mass spectrometric measurements for nitric oxide density calculations and missing coordinated measurements of temperature, turbulence and horizontal winds, it was not yet possible to demonstrate directly the nitric oxide density variability by transport in the lower thermosphere and mesosphere.

The source for the nitric oxide of salvo B and A2 was mainly $N(^2D)$ and $N(^4S)$ produced by precipitated electrons and protons. The altitudes of the derived maximum nitric oxide density values are near or at the height of maximum ion-electron pair production (Ref. 6). The model of the nitric oxide production through reactions of $N(^2D)$ and $N(^4S)$ with O_2 and NO predict only a slight negative temperature dependence in the lower thermosphere by reaction $N(^4S) + NO \rightarrow N_2 + O$. A value of $1.5 \times 10^{-12}\sqrt{T}$ is used in the model by Gérard and Barth (Ref. 14) for this reaction. The effect of a temperature controlled loss of nitric oxide by $N(^4S)$ could explain the slight density variation in the altitude region 110 - 120 km of salvo B (Fig. 2).

The comparison of the total horizontal wind velocity from the falling sphere experiment and the nitric oxide density in salvo B and A2 (Figs. 2 and 3) shows that the mesospheric density minimum of nitric oxide at 97 km and 93 km respectively is located exactly at the altitude of maximum horizontal wind velocity measured with the falling sphere experiment. This maximum horizontal wind velocity is mainly the W-E wind component in salvo B and the S-N wind component in salvo A2. The large and variable horizontal wind field is thus a determining factor for the vertical mesospheric density profile of nitric oxide at high latitudes under auroral conditions. It is also interesting to note that despite the time difference of 57 min and 24 min between the ion composition measurement of the E11-A payload and the falling sphere experiment of the E6-A payload in salvo B and A2 respectively, the altitude correlation between the mesospheric NO minimum and maximum horizontal wind velocity is still good and indicates a large spacial variability of the nitric oxide density in the mesosphere. The nitric oxide variability of the mesosphere is determined by the following two reasons:

1. Local variability of the downward transport of nitric oxide.

2. The nitric oxide production by energetic particles at mesospheric heights is reduced and much more variable in space and time compared to the region of maximum production between 100 - 130 km.

5. TEMPERATURE

The positive ion composition in the D-region is characterized by the presence of oxonium hydrates named proton hydrates $H^+(H_2O)_n$ with different hydration degrees. The occurrence of these ions at altitudes below about 80 km is due to the presence of water vapor in the middle atmosphere and to the large proton affinity of water and the strong bonding of this molecule to oxonium ion H_3O^+. The transition of proton hydrates to the molecular ions NO^+ and O_2^+ occurs within a relatively narrow altitude region of the order of a few kilometers. The first three proton hydrates $H^+(H_2O)_{1-3}$ are formed over a set of chemical reactions starting from NO^+ and O_2^+. Higher order proton hydrates ($n > 3$) are then produced by three body reactions with water vapor

$$H^+(H_2O)_n + H_2O + M \rightleftarrows H^+(H_2O)_{n+1} + M \qquad (1)$$

$(M = O_2, N_2)$

The stability of higher order proton hydrates is a function of temperature due to possible thermal break-up reactions after a collision. This is in agreement with the trend of decreasing stability of the proton hydrates with increasing hydration order. Measurements of higher order proton hydrates of mass 91, 109 and 127 amu from summer mid- and high-latitude rocket flight flights are connected to the seasonal mesospheric temperature decrease in summer.

The application of the equilibrium constants of reaction (1) measured by Kebarle et al. (Ref. 15) in the general D-region ion chemical reaction scheme by Reid (Ref. 16), can be used to infer temperature values from the measured proton hydrate ion distribution of the D-region. Fig. 4 gives the temperatures derived from the density ratio $H^+(H_2O)_4 / H^+(H_2O)_3$ of the mass spectrometric measurements on the E11-A payload

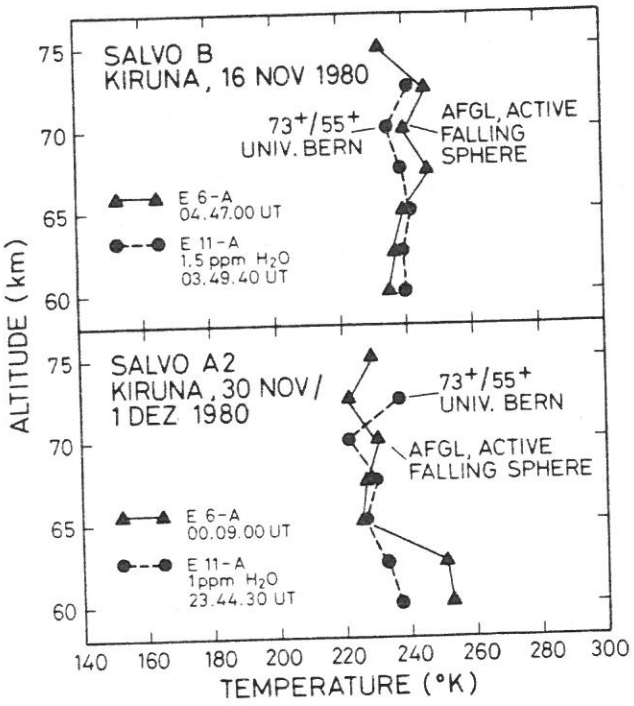

Fig. 4: Temperature of the lower mesosphere obtained from model calculations of the positive ion composition measurements and the falling sphere experiment of salvo B and A2.

in salvo B and A2. The tmeperature values were derived with a water vapor mixing of 1.5 ppm for salvo B and 1 ppm for salvo A2. These values are taken from typical values for salvo B and A2 published by Grossmann et al. (Ref. 17). The derived temperature of salvo B is around 240 K and between 220 - 240 K in salvo A2. Both flights show good temperature agreement with the falling sphere results in the altitude range 60 - 73 km. The temperature derived from the proton hydrate distribution is almost independent to the variation of the water vapor mixing ratio. The difference between the two temperature profiles of Fig. 4 may in fact also come from a natural time variability between the two rocket flights E11-A and E6-A. The application of Kebarle's equilibrium constants for reaction (1) measured at room temperatures seem to give good results also at 200 - 240 K. It is however doubtful whether these values can also be used for extreme mesospheric temperatures in summer at high latitudes around or below 140 K.

6. ACKNOWLEDGEMENTS

One of us (E. Kopp) is supported by the Swiss National Science Foundation through grants 2.255.81 and 2.609.82.

Mass.

7. REFERENCES

1. Arnold, F. (1980), The middle atmosphere ionized component, ESA SP-152-June 1980, 479-496.

2. Cravens, T.E. and A.I. Stewart (1978), Global morphology of nitric oxide in the lower E-region, J. Geophys. Res. 83, 2446-2452.

3. Solomon, S., P.J. Crutzen and R.G. Roble (1982), Photochemical coupling between the thermosphere and the lower atmosphere, 1. Odd nitrogen from 50 to 120 km, J. Geophys. Res. 87, 7206-7220.

4. Megie, G., F. Bos, J.E. Blamont and M.L. Chanin (1978), Simultaneous nighttime lidar measurements of atmospheric sodium and potassium, Planet. Space Sci. 26, 27-35.

5. Garcia, R.R., S. Solomon (1983), A numerical model of the zonally averaged dynamical and chemical structure of the middle atmosphere, J. Geophys. Res. 88, 1379-1400.

6. Kopp, E., L. André and L.G. Smith (1983), Positive ion composition and derived particle heating in the lower auroral ionosphere, to be published in J. Atmos. Terr. Phys.

7. Schmidlin, F.J., M. Carlson, D. Offermann, C.R. Philbrick, D. Rees and H.U. Widdel (1983), Wind structure and small-scale wind variability in the stratosphere and mesosphere during the November 1980 Energy Budget Campaign, to be published in J. Atmos. Terr. Phys.

8. Philbrick, C.R., R. Henning, G. Lange, D. Krankowsky, F.J. Schmidlin and U. von Zahn (1983), Vertical density and temperature structure over Northern Europe, to be published in J. Atmos. Terr. Phys.

9. Kopp, E., L. André, P. Eberhardt and U. Herrmann (1981), Mass spectrometer for ion composition measurements in the lower ionosphere, BMFT-FB-W81-052, p. 416-423, Universtiy of Wuppertal Physics Department, Wuppertal.

10. Philbrick, C.R., J.R. McIsaac, D.H. Fryklund and R.F. Buck (1981), Atmospheric structure measurements from accelerometer instrumented falling spheres, BMFT-FB-W81-052, p. 352-361, University of Wuppertal, Physics Department, Wuppertal.

11. Swider, W. and R.S. Narcisi (1977), Auroral E-region: Ion composition and

12. Von Zahn, U., K.D. Baker and P.H.G. Dickinson (1983), Lower thermosphere densities of N_2, O and Ar under high latitude winter conditions, to be published in J. Atmos. Terr. Phys.

13. Swider, W. (1978), Daytime nitric oxide at the base of the thermosphere, J. Geophys. Res. 83, 4407-4410.

14. Gérard, J.-C and C.A. Barth (1977), High-latitude nitric oxide in the lower thermosphere, J. Geophys. Res. 82, 674-680.

15. Kebarle, P., S.K. Searles, A. Zolla, J. Scarborough and M. Arshadi (1967), The solvation of the hydrogen ion by water molecules in the gas phase. Heats and entropies of solvation of individual reactions: $H^+(H_2O)_{n-1} + H_2O \rightarrow H^+(H_2O)_n$, Am. Chem. Soc. J. 89, 6393-6399.

16. Reid, C.G. (1977), Ion chemistry in the D-region, in Book Adv. At. Mole. Phys. 12, 375-413, Ed. D.R. Bates and B. Bederson, Academic Press, New York/ London.

17. Grossmann, K.U., W.G. Frings, D. Offermann, L. André, E. Kopp and D. Krankowsky (1983), Concentration of H_2O and NO in mesosphere and lower thermosphere at high latitudes, to be published in J. Atmos. Terr. Phys.